CSF 5703600 MASTER COPY KEEP FOR REPRODUCTION PURPOSES

REPORT DOCUMENTATION PAGE

Form Approved OMB NO. 0704-0188

1. AGENCY USE ONLY *(Leave blank)*	2. REPORT DATE	3. REPORT TYPE AND DATES COVERED
	5/15/02	Final Progress 6/1/98 - 12/31/01

4. TITLE AND SUBTITLE

Quantum Computation with Mesoscopic Superconducting Devices

5. FUNDING NUMBERS

DAAG55-98-1-0369

6. AUTHOR(S)

Prof. Terry P. Orlando

7. PERFORMING ORGANIZATION NAMES(S) AND ADDRESS(ES)

Massachusetts Institute of Technology
Research Laboratory of Electronics
77 Massachusetts Avenue
Cambridge, MA 02139-4307

8. PERFORMING ORGANIZATION REPORT NUMBER

9. SPONSORING / MONITORING AGENCY NAME(S) AND ADDRESS(ES)

U.S. Army Research Office
P.O. Box 12211
Research Triangle Park, NC 27709-2211

10. SPONSORING / MONITORING AGENCY REPORT NUMBER

P-38809-PH-QC

11. SUPPLEMENTARY NOTES

The views, opinions and/or findings contained in this report are those of the author(s) and should not be construed as an official Department of the Army position, policy or decision, unless so designated by other documentation.

12a. DISTRIBUTION / AVAILABILITY STATEMENT

Approved for public release; distribution unlimited.

12 b. DISTRIBUTION CODE

13. ABSTRACT *(Maximum 200 words)*

The goal of this research was to explore the use of superconducting circuits as components for quantum computing. Quantum computers are devices that store information on quantum variables and process that information by making those variables interact in a way that preserves quantum coherence. Typically, these variables consist of two quantum states, and the quantum device is called a quantum bit or qubit. Superconducting quantum circuits have been proposed as qubits, in which circulating currents of opposite polarity characterize the two quantum states. Recent experiments show that these two macroscopic quantum states can be put into a superposition. In particular, microwave spectroscopy experiments indicate symmetric and anti-symmetric quantum superpositions of macroscopic states.

14. SUBJECT TERMS

15. NUMBER IF PAGES

16. PRICE CODE

17. SECURITY CLASSIFICATION OR REPORT	18. SECURITY CLASSIFICATION OF THIS PAGE	19. SECURITY CLASSIFICATION OF ABSTRACT	20. LIMITATION OF ABSTRACT
UNCLASSIFIED	UNCLASSIFIED	UNCLASSIFIED	UL

Final Report for "Quantum Computation with Mesoscopic Superconducting Devices" DAAG55-98-1-0369

T. P. Orlando, J. E. Mooij, and Seth Lloyd
Massachusetts Institute of Technology

2. Contents

3. List of Appendices, Illustrations and Tables

4. Statement of the problem studied:

The goal of this research was to explore the use of superconducting circuits as components for quantum computing. Quantum computers are devices that store information on quantum variables and process that information by making those variables interact in a way that preserves quantum coherence. Typically, these variables consist of two quantum states, and the quantum device is called a quantum bit or qubit. Superconducting quantum circuits have been proposed as qubits, in which circulating currents of opposite polarity characterize the two quantum states. Recent experiments show that these two macroscopic quantum states can be put into a superposition. In particular, microwave spectroscopy experiments indicate symmetric and anti-symmetric quantum superpositions of macroscopic states.

This research focused on using superconducting quantum circuits to perform the measurement process and to model the sources of decoherence.

5. Summary of Important Results

5.1. Superconducting Persistent Current Qubits In Aluminum

Quantum computers are devices that store information on quantum variables such as spin, photons, and atoms, and process that information by making those variables interact in a way that preserves quantum coherence. Typically, these variables consist of two-state quantum systems called quantum bits or 'qubits'. To perform a quantum computation, one must be able to prepare qubits in a desired initial state, coherently manipulate superpositions of a qubit's two states, couple qubits together, measure their state, and keep them relatively free from interactions that induce noise and decoherence.

We have designed a superconducting qubit that has circulating currents of opposite sign as its two states. The circuit consists of three nano-scale aluminum Josephson junctions connected in a superconducting loop and controlled by magnetic fields.

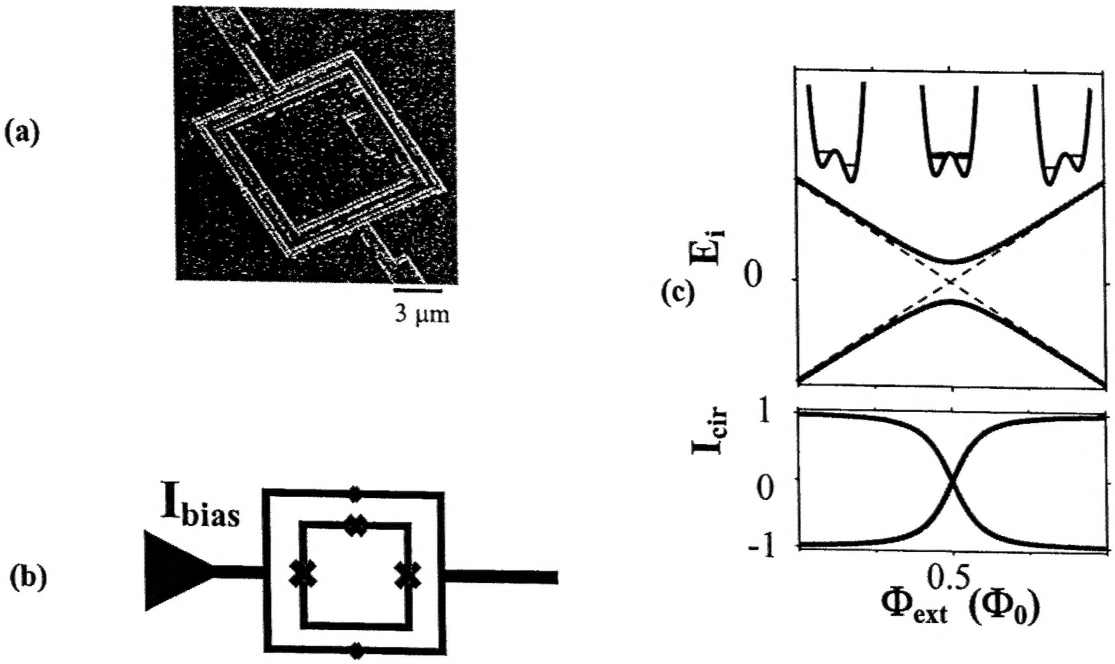

FIGURE 1. (a) SEM image of the persistent current qubit (inner loop) surrounded by the measuring dc SQUID. (b) a schematic of the qubit and measuring SQUID, the x's mark the Josephson junctions. (c) The energy levels for the ground state (dark line) and the first excited state of the qubit versus applied flux. The double well potentials are shown schematically above. The lower graph shows the circulating current in the qubit for both states as a function of applied flux. The units of flux are given in terms of the flux quantum.

Figure 1a shows a SEM image of the persistent current qubit (inner loop) and the measuring dc SQUID (outer) loop. The Josephson junctions appear as small "breaks" in the image. A schematic of the qubit and the measuring circuit is shown in Figure 1b, where the Josephson junctions are denoted by x's. The qubit loop is 5×5 μm^2 with aluminum-oxide tunnel junctions, microfabricated at the TU Delft, by a shadow evaporation technique. (This is in contrast to the samples fabricated at MIT's Lincoln Laboratory that are made in niobium by photolithographic techniques on a trilayer of niobium-aluminum oxide-niobium wafer.) The capacitance of the junction is estimated to be about 3 fF and the ratio of the Josephson energy to the charging energy is about 40. The inductances of the inner qubit loop and the outer measuring loop are about 11 and 16 pH respectively, with a 7 pH mutual inductive coupling.

The energy levels of the ground state (dark line) and the first excited state (light line) are shown in Figure 1c near the applied magnetic field of 0.5 Φ_0 in the qubit loop. Classically the Josephson energy of the two states would be degenerate at this bias magnetic field and increase and decrease linearly from this bias field, as shown by the dotted line. Since the slope of the E versus magnetic field is the circulating current, we see that these two classical states have opposite circulating currents. However, quantum mechanically, the charging energy couples these two states and results in a energy level repulsion at $\Phi_{ext} = 0.5\ \Phi_0$, so that there the system is in a linear superposition of the currents flowing in opposite directions. As the applied field is

changed from below $\Phi_{ext} = 0.5\ \Phi_0$ to above, we see that the circulating current goes from negative, to zero at $\Phi_{ext} = 0.5\ \Phi_0$, to positive as shown in the lower graph of Figure 1c. This flux can be measured by the sensitive flux meter provided by the dc SQUID.

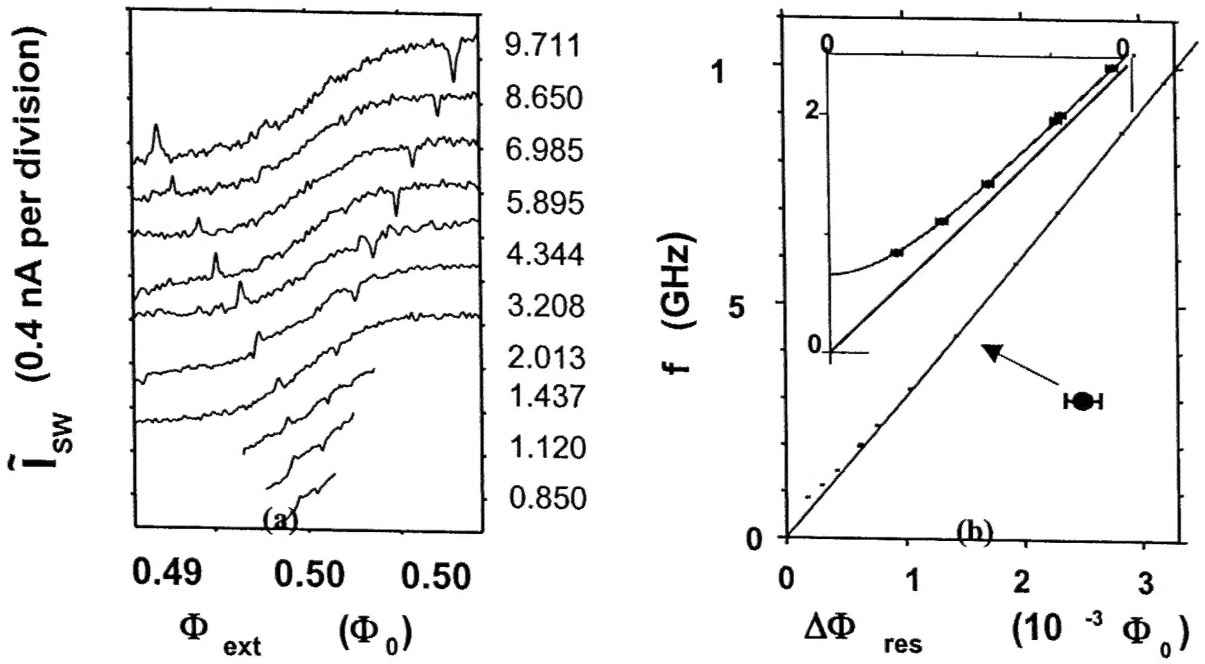

FIGURE 2. (a) The circulating current as inferred from the dc SQUID measurements for various applied microwave frequencies. The curves are offset for clarity. (b) Half the distance in Φ_{ext} measured between the resonant peaks and the dips at different frequencies *f*. The inset shows the low frequency data points. The grey line is a linear fit through the high frequency points and zero. The black line is a fit of the quantum theory.

Figure 2a shows the circulating current as inferred from the dc SQUID measurements for various applied microwave frequencies. The curves are offset for clarity, and each curve shows the expected change from negative circulating current at low applied flux, to zero at half a flux quantum, and then to positive current at higher flux. This clearly shows that the qubit has the change in flux profile expected of the ground state. When microwaves are applied at the energy difference matching the difference between the ground state and the first excited state, then a transition is induced from the ground state to the first excited state. These are shown by the resonant-like structures in each curve. A plot of the distance in Φ_{ext} at the resonance from $\Phi_{ext} = 0.5\ \Phi_0$ is shown in the figure on the left. Quantum mechanically the energy is expected to follow the form

$$\Delta E = \sqrt{\left[2I_p\left(\Phi_{ext} - 0.5\Phi_0\right)\right]^2 + \left(2V\right)^2}$$

where I_p is the circulating current and V is the tunneling matrix element between the two circulating current states at $\Phi_{ext} = 0.5\ \Phi_0$. The inset shows a fit to the curve which gives an energy gap of about 600 MHz and a circulating current of about 500 nA as expected. These results are among the first experimental verification of the superposition of macroscopic circulating current states.

5.2 Superconducting Persistent Current Qubits in Niobium

The particular device that we have studied so far is made from a loop of Nb interrupted by 3 Josephson junctions. The application of an external magnetic field to the loop induces a circulating current whose magnetic field either adds to (say circulating current in the clockwise direction) or opposes (counterclockwise) the applied magnetic field. When the applied field is near to one-half of a flux quantum, both the clockwise and counterclockwise current states are classically stable. The system behaves as a two-state system. The potential energy versus circulating current is a so-called double-well potential, with the two minima representing the two states of equal and opposite circulating current. A SQUID magnetometer inductively coupled to the qubit can be used to measure the magnetic field caused by the circulating current and thus determine the state of the qubit. The SQUID has a switching current which depends very sensitively on magnetic field. When the magnetic field from the qubit adds to the external field we observe a smaller switching current; when it subtracts from the external field we observe a smaller larger current. We measure the switching current by ramping up the bias current of the SQUID and recording the current at which it switches. Typically a few hundred such measurements are taken. We have performed these measurements versus magnetic field, temperature and SQUID ramping rate.

In the upper plot of Fig. 1 we show the average switching current versus magnetic field for our qubit-SQUID system. The SQUID switching current depends linearly on the applied magnetic field. A step-like transition occurs when the circulating current in the qubit changes sign, hence changing whether its magnetic field adds to or subtracts from the applied field. In Fig. 1 the qubit field adds to the SQUID switching current at lower fields (< 3mG) but subtracts from it at higher fields (>3mG). Each point in the upper curve is an average of 1000 single switching current measurements. If we look at a histogram of the 1000 switching currents in the neighborhood of the transition, we discover that it represents a joint probability distribution. Two distinct switching currents representing the two states of the qubit can be clearly resolved. Changing the magnetic field alters the probability of being measured in one state or the other.

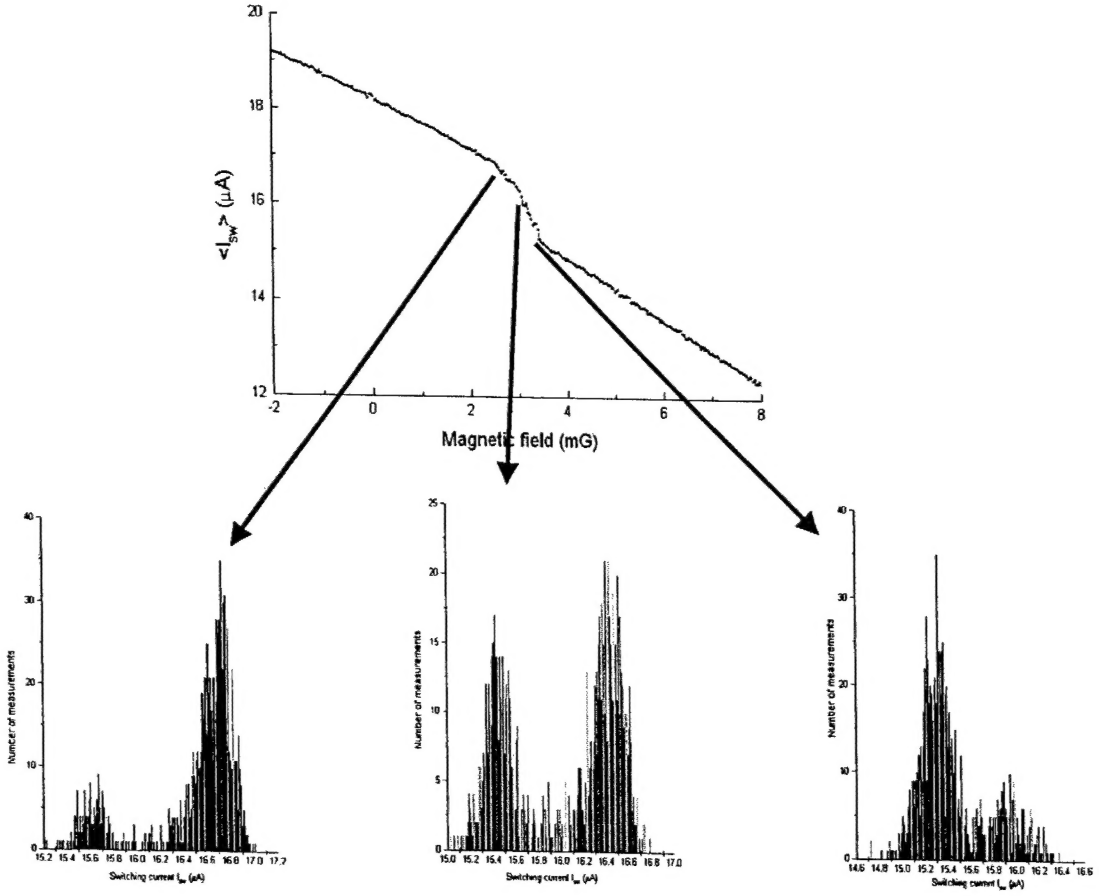

Fig. 1: Measurements of the switching current of the SQUID versus magnetic field.

5.3 Integrated Superconducting Device Technology for Qubit Control

Personnel

D. Nakada, M. O'Hara, K. Berggren[1], T. Weir[1], E. Macedo[1], and R. Slattery[1] (T. P. Orlando)

Sponsorship

NSA and ARDA under ARO Grant DAAG55-98-1-0369
Lincoln Laboratory New Technology Initiative Program

Quantum computing requires the time-dependent control and readout of qubit couplings. Critical to the project of quantum computing is therefore the integration of quantum devices with conventional superconducting digital and analog electronics that will be used to provide classical circuitry for control and readout functions of the quantum computer. The "classical" and "quantum" devices can be integrated using inductive coupling between chips bonded by a flip-chip process. There exists a classical electronics family based on superconductive electronics-Single Flux Quantum (SFQ) logic – having the capability of operating well above 100GHz clock speeds. Such devices can be used to execute many control operations before substantial decoherence occurs in the persistent current qubit – a feature that could benefit other solid-state qubit technologies with long coherence times. The flip-chip process is not limited to the field of

quantum computing but has applications in any technology that would benefit from SFQ electronics.

We have designed experiments to couple current magnetically from a carrier chip, onto a flipped chip (Figure 3), and back onto a different area of the carrier chip where the resulting magnetic field was sensed with a dc SQUID. The flipped chip lies less than 2μm above the carrier chip with less than 2μm of linear misalignment. The magnetic coupling between the current line and dc SQUID was enhanced due to the presence of a transformer loop on the flipped chip. To show this, we compared the effective mutual inductance between the control current and the dc SQUID with and without the presence of the flipped-chip. For quantum computing implementation, the flipped chip would carry the qubits while the carrier chip will contain the control and readout circuitry for determining the state of the qubit.

5.4 Resonant Cancellation of Off-resonant Transitions in a Multilevel Qubit

Personnel
L. Tian, S. Lloyd, J.E. Mooij[1], F.K. Wilhelm[1](T.P. Orlando)

Sponsorship
NSA and ARDA under ARO Grant DAAG55-98-1-0369

Off-resonant effects are a significant source of error in quantum computation. Physical qubits are not ideal two level systems, but have many higher levels that are irrelevant for the qubit operation. The off-resonant transitions to the higher levels of a qubit during a gate operation is a particularly important form of intrinsic qubit error. Numerical simulation shows that this effect can introduce an error amplitude as high as 1% in the superconducting persistent current qubit, which is significantly higher than the noise from environmental fluctuations of the qubit.

To correct this error and accomplish quantum computation, we study the effect of the higher levels on qubit dynamics during qubit operation by a group theory approach. We prove that the errors can be completely avoided by applying a time varying operation Hamiltonian. The transformations on an N-level quantum system are described by the N^2 dimensional compact Lie group $U(N)$. By applying controllable pulses of Hamiltonian H_I, with $[H_0, H_I]$, any transformation in $U(N)$ can be reached within N^2 number of pulses. This shows that the transformation on a given quantum system can be restricted to the lowest two levels with time varying pumping.

[1] *Delft University of Technology, The Netherlands*
This study was then generalized to the qubit error resulting from the interaction between different qubits. Qubit interaction is necessary for operations such as a CNOT gate that is necessary for the universal set of quantum gates of quantum computation. But qubit interaction also introduces operational errors by additional transition matrix elements during gate operations. By mapping the interacting qubits as a multilevel quantum system with higher levels, the same method can be applied to correct the errors in the coupled qubit system.

By extending the idea of dynamic pulse control by Viola and Lloyd, we designed a pulse sequence that cancels the leakage to the higher levels to arbitrary accuracy with $O(N)$ number of pulses, N being the number of higher levels. This approach exploits 'bang-bang' control techniques where the dynamics of the qubit and its environment is manipulated by fast pulses that flip the qubit state. With the influence of the environment being averaged out, the qubit evolves in the error-free subspace. This method relies on the ability to apply the pulses rapidly compared with the correlation time of the environment. This is an open loop control method.

In the proposed method, we apply resonant pulses between different eigen-levels to cancel the unwanted off-resonant transitions to the higher levels. All the pulses applied have the same time duration. By adjusting the amplitudes and phases of the pulses, the leakage to higher levels can be completely suppressed at the end of the operation. Since all the pulses in this sequence have the same pulse length, they can be combined into one pulse with slightly different parameters. This method for protecting quantum information is complementary to quantum error correcting codes and the 'bang-bang' technique mentioned above. Like the bang-bang method, it has the advantage that it does not require extra qubits to enact. The proposed method protects against a different class of errors from those corrected by the methods of Viola, however. Dynamic pulse control can be used in conjunction with quantum error correcting codes and bang-bang decoupling methods.

5.5 Relaxation of a Coherent Quantum System During Premeasurement Entanglement

Personnel

L. Tian, S. Lloyd, J.E. Mooij[1], F.K. Wilhelm[1], C.H. van der Wal[1], and L. Levitov (T.P. Orlando)

Sponsorship

NSA and ARDA under ARO Grant DAAG55-98-1-0369

Recent experiments on superconducting loops have demonstrated macroscopic quantum effects. These experiments used a dc SQUID to measure the magnetic flux generated by the persistent currents of the macroscopic quantum states. Due to the inductive interaction between the qubit and the SQUID, the relaxation and dephasing of the qubit are limited by the entanglement with the measurement device as well as its coupling to the solid-state environment. We studied the effect of the meter (SQUID) environmental spectrum density on the qubit dynamics within the

[1] *Delft University of Technology, The Netherlands*

spin-boson formalism. The results can be applied to optimizing the measurement circuit for the best measurement efficiency.

As the ramping current to the dc SQUID increases, the interaction between the qubit and the dc SQUID entangles the qubit state and the SQUID state. This entanglement brings indirect interaction between the qubit and the SQUID environment and introduces additional noise to the qubit. As this interaction does not commute with the qubit Hamiltonian, it influences the qubit dynamics non-trivially. The effective spectrum density seen by the qubit is renormalized due to the presence of the meter degrees of freedom and has a different shape from the spectrum density seen by the meter.

The qubit dynamics can be described within the master equation approach when the interaction with the environment is weak. From this approach the relaxation and decoherence of the qubit, also called the transversal relaxation and the longitudinal relaxation rates, are described by the spectrum density of the environment. As the inductive interaction induces a σ_z interaction between the qubit and SQUID environment, the qubit Hamiltonian H_0 has non-commuting σ_x component with the σ_z interaction, a transversal interaction that flips the qubit and eventually relaxes the it in the qubit eigen basis is created. This transversal interaction depends on both the tunneling between the two localized qubit states and the inductance coupling quadratically. With the renormalized spectrum density, the qubit is damped strongly by the SQUID environment. This effect prevents the measurement of the coherent oscillation between the macroscopic states with the current experimental setup.

Our study also suggests that by engineering the measurement circuit, we can optimize the spectrum density seen by the qubit and minimize the relaxation of the qubit due to various environmental fluctuations. Within the theoretical framework, various designs can be analyzed and compared.

5.6 Inductance effects in the Persistent Current Qubit

Personnel
D.S. Crankshaw (T.P. Orlando)

Sponsorship
NSA and ARDA under ARO Grant DAAG55-98-1-0369

In the original description of the persistent current qubit, the inductance was neglected in the energy level calculations. The effects of the small inductance in the PC qubit can be included by using a perturbative approach. This technique simplifies the numerical calculations by reducing the dimensionality of the Schrödinger equation that must be solved. Consider a circuit with b branches, each with a Josephson junction, connected at n nodes to form m meshes (loops). In general, the dimensionality of the Schrödinger equation for such a circuit is $b=n+m-1$. If the inductance of each mesh is small so that $\beta_L<<1$, the energy levels can be calculated by ignoring the inductances (i.e., setting $\beta_L=0$). The dimensionality of the resulting Schrödinger equation is the number of independent nodes n -1 < b. Moreover, we find that the Hamiltonian can be written in the form

$$H_b = H_n(\Theta_n) + H_m(I_m) + \Delta H(\langle\Theta_n\rangle, \langle I_m\rangle)\,. \tag{2}$$

The full Hamiltonian, H_b, of b variables is written in terms of three Hamiltonians: the first, $H_n(\Theta_n)$, is of the form of what one would write with $\beta_L=0$, and has n-1 node variables Θ_n. $H_n(\Theta_n)$ is periodic in each of these variables. The second, $H_m(I_m)$, is of the form of a simple harmonic oscillator of the m mesh (circulating) current variables. The last term is a correction term that can often be neglected in calculating the energy levels. If we can separate the Hamiltonian this way, the mesh Hamiltonian and the correction term are easily solved analytically (since one is a

simple harmonic oscillator and the other is calculated from the expectation values of the other Hamiltonians' variables), leaving only the node Hamiltonian, which has a lower dimensionality than the branch Hamiltonian and is periodic in all its variables. This is solved numerically. (This reduces the computational time of $O(N^b)$ for H_b to $O(N^{n-1})$, $O(m)$, and $O(nN+m)$ for the terms H_n, H_m, and ΔH respectively, where N is the number of discretized elements of the quantum phase variables.)

When the qubit is modeled in a way to facilitate this derivation (see Figure 4), it reduces to the simplified equation

$$E = E_q(f) + (n+\tfrac{1}{2})\hbar\omega_0 - \tfrac{1}{2}L_m I_c^2\left(\frac{\alpha}{1+2\alpha}\right)^2\left(\left\langle \sin\left(2\tilde{\Theta}_m + 2\pi f\right)\right\rangle - \left\langle 2\cos\Theta_p \sin\tilde{\Theta}_m\right\rangle\right)^2. \quad (3)$$

The first term is the original, zero inductance solution to the qubit energy, the second term is the harmonic oscillator of the circulating current variables, and the final term is the correction term. The result for a realistic value of the qubit inductance is shown in Figure 4, which indicates that the deviation from the zero inductance solution in negligible.

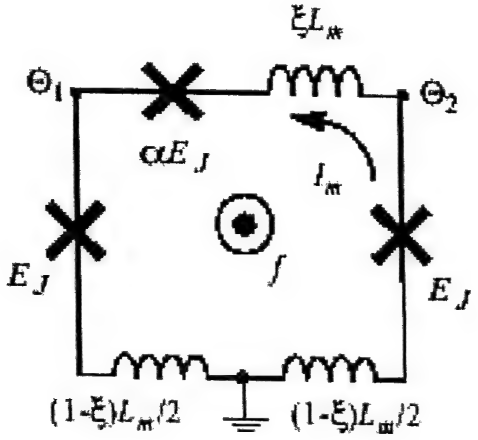

5.7 Decoherence of an On-Chip Oscillator

The two devices which have the most intimate connection to the qubit are the proposed on-chip oscillator and the DC SQUID. Designing these devices requires not just concern for proper operation, but for minimum decoherence as well.

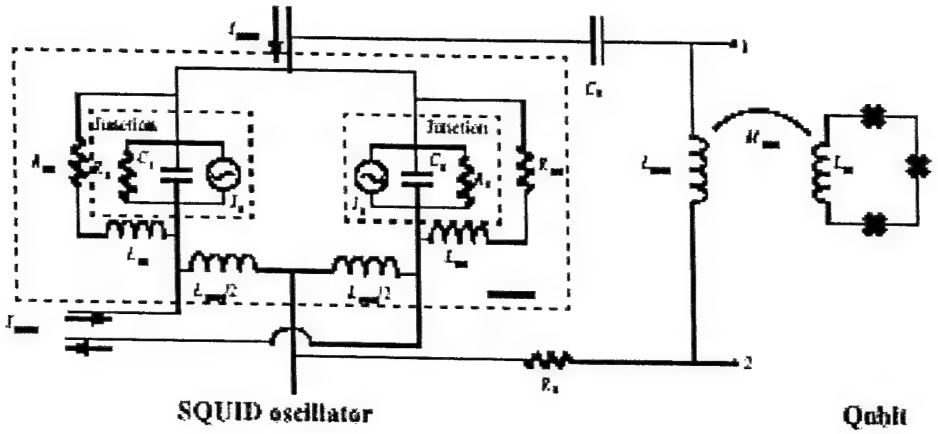

FIGURE 1. Circuit diagram of the SQUID oscillator coupled to the qubit. The SQUID contains two identical junctions, here represented as independent current sources and the RCSJ model, shunted by a resistor and inductor (R_{sh} and L_{sh}). A large superconducting loop (L_{mw}) provides the coupling to the qubit. The capacitor, C_c, prevents the DC current from flowing through this line, and the resistance, R_c, damps the resonance. Z_t, the impedance seen by the qubit, is the impedance across the inductor, Z_{12}.

The oscillator in Figure 1 is a simple overdamped DC SQUID. This gives two parameters with which to control the frequency and amplitude of the source: the bias current and the magnetic flux through the SQUID. In this design, the SQUID is placed on a ground plane to minimize any field bias from an external source, and direct injection supplies the flux by producing excess current along a portion of the SQUID loop. When a Josephson junction is voltage biased, its current oscillates at a frequency of $V_{bias}/\Phi$with an amplitude of I_c. For a stable voltage bias, this looks like an independent AC current source. In this circuit, the junction is current biased, and its oscillating output produces fluctuations in the voltage across the junction. Thus the DC voltage, approximately equal to *IbiasRsh*, gives the fundamental frequency, while harmonics distort the signal. If the shunt is small, such that $V_{bias}>>I_c|R_{sh}+j\omega L_{sh}|$, the voltage oscillations are small relative to the DC voltage and the higher harmonics become less of a problem. This allows us to model the junctions as independent sources (I_0 and I_1) in parallel with the RCSJ model. A DC SQUID with a small self inductance behaves much like a single junction whose I_c can be controlled by the flux through its loop. The circuit model is shown in Figure 1. This is similar in concept to our previous work with array oscillators. The impedance seen by the qubit is given by:

$$Z_t(\omega)=\left[\left(\frac{1/2}{j\omega C_j+\frac{1}{R_n}+\frac{1}{R_{sh}+j\omega L_{sh}}}+\frac{1}{j\omega C_c}+R_c\right)^{-1}+\frac{1}{j\omega L_{mw}}\right]^{-1}$$

This value comes from placing the other elements of the circuit in parallel with the inductance. The maximum amplitude of the oscillating magnetic flux is at the resonance of the RLC circuit consisting of R_c, C_c, and L_{mw}. In this case, the LC resonance occurs at 8.6 GHz. Directly on resonance, the SQUID produces high amplitude oscillations with a short dephasing time. Moving it off resonance lowers the amplitude but lengthens the dephasing time, as shown in Figure 2.

Table 1. SQUID oscillator parameters

I_c	R_n	C_j	R_{sh}	L_{sh}	R_c	C_c	L_{mw}	M_{mw}
260 μA	7.3 Ω	2100 fF	0.19 Ω	0.38 pH	0.73 Ω	4600 fF	75 pH	0.6 pH

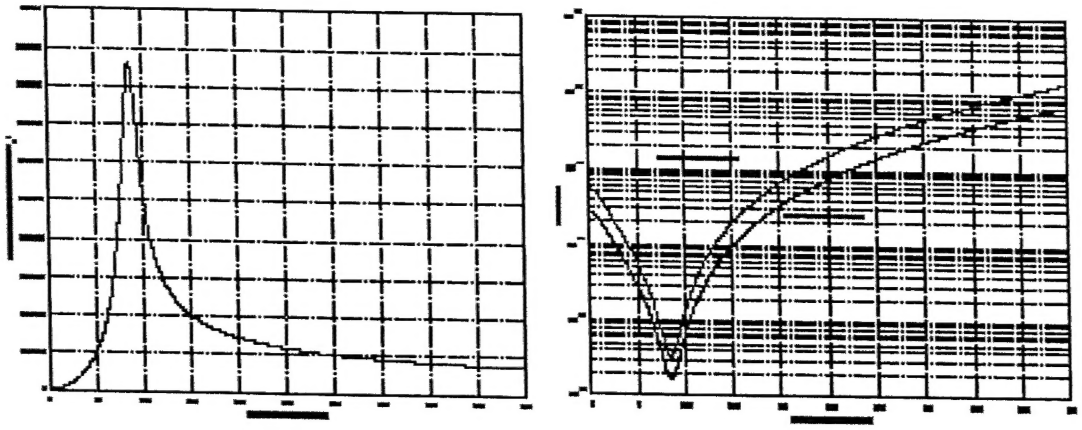

(a) (b)

FIGURE 2. Graphs showing the amplitude produced by the oscillator (a) and the decoherence times caused by the oscillator (b) as a function of frequency.

The noise from the DC SQUID shown in Figure 3 has a more complex relationship with the qubit decoherence. Since the resistive noise source is located outside of the SQUID, the noise contribution is evenly divided between the two branches. As the bias current is increased, however, the combination of circulating current and bias current creates different linear characteristics in the branches. The internal phase variable, $\varphi_{int}=(\varphi_1-\varphi_2)/2$, is driven by the external flux, so that $\varphi_{int}=\pi\Phi\Phi 0$. This is considered a constant. φ_{ext} follows the bias current. While *I cir* directly couples to the qubit, environmental noise appears as fluctuations in the *I bias*. The fluctuations in *I bias* can be translated into fluctuations of *I cir* through Equation (2).

$$\delta I_{bias} = 2I_{c0}\cos\varphi_{\text{int}}\cos\overline{\varphi}_{ext}\delta\varphi_{ext}$$
$$\delta I_{cir} = I_{c0}\sin\varphi_{\text{int}}\sin\overline{\varphi}_{ext}\delta\varphi_{ext}$$

By translating the noise seen on the external phase variable into noise in the circulating current, which couples to the qubit, we can derive the spectral density in Equation (3), from which we derive decoherence and dephasing times.

$$J(\omega)=\left(\frac{2e}{\hbar}\right)^2\frac{4}{\hbar\omega}\left(MI_pI_{bias}\tan\varphi_{\text{int}}\right)^2\Re\{Z_t(\omega)\}$$

$Z_t(\omega)$ the impedance of the external environment. This is very similar to the above use of $Z_t(\omega)$, where it was the external environment seen across the inductor, except that in this case, the external environment includes the SQUID itself (its Josephson inductance and capacitance must be included, along with any external capacitance and resistance from the environment). Notice that the decoherence caused by the SQUID increases with its bias current. Thus, when the SQUID is unbiased, it should not contribute to decoherence at all.

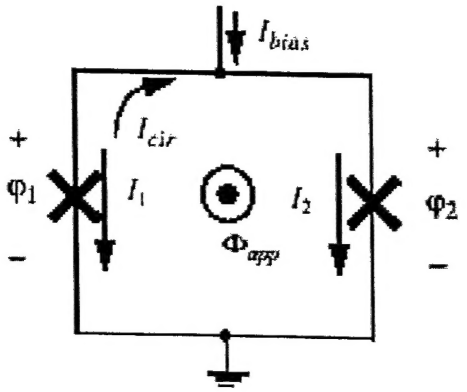

FIGURE 3. Circuit diagram of the DC SQUID.

6. Publications

C.H. van der Wal, A.C.J. ter Haar, F.K. Wilhelm, R.N. Schouten, C.J.P.M. Harmans, T. P. Orlando, Seth Lloyd, J. E. Mooij, "Quantum Superposition of Macroscopic Persistent-Current States," *Science* **290**, 773-777 (2000).

L. Tian, L. Levitov, C.H. van der Wal, J.E. Mooij, T.P. Orlando, S. Lloyd, C.J.P.M. Harmans, J.J. Mazo, "Decoherence of the superconducting persistent current qubit," *Quantum Mesoscopic Phenomena and Mesoscopic Devices in Microelectronics* edited by I. O. Kulik and R. Ellialogulu, Kluwer, (2000).

E. Trías, J.J. Mazo, T.P. Orlando, "Discrete breathers in nonlinear lattices: Experimental detection in a Josephson array," *Phys. Rev. Letts.* **84**, 741-744, (2000).

E. Trías, J.J. Mazo, F. Falo, and T. P. Orlando, "Depinning of kinks in a Josephson-junction ratchet array," *Phys. Rev. E* **61**, 2257---2266, (2000).

D.S. Crankshaw, E. Trías, T.P. Orlando, "Tunable Power Output of a Parallel Array of Overdamped Josephson Junction," to be published in the *IEEE Trans. on Applied Superconductivity*.

T. P. Orlando, S. Lloyd, L. S. Levitov, K. K. Berggren, M. J. Feldman, M. F. Bocko, J. E. Mooij, C. J. P. Harmans, C. H. van der Wal, "Flux-based Superconducting Qubits for Quantum Computation," presented at the 5th European Conference on Applied Superconductivity, Copenhagen, August 2001.

T. P. Orlando, Lin Tian, D. S. Crankshaw, S. Lloyd, C. H. van der Wal, J. E. Mooij, F. Wilhelm, "Engineering the Quantum Measurement Process for the Persistent Current Qubit," presented at SQUID 2001, Sweden, August 2001.

D. S. Crankshaw, T. P. Orlando, "Coherent Driving of the Persistent Current Qubit,"

D. S. Crankshaw and T. P. Orlando, "Inductance effects in the persistent current qubit," *IEEE Trans. on Applied Superconductivity:* Volume: 11 Issue: 1 Part: 1 p: 1006 -1009, March 2001

D.S. Crankshaw, E. Trias, T.P. Orlando, "Magnetic flux controlled Josephson array oscillators," *IEEE Transactions on Applied Superconductivity,* Volume: 11 Issue: 1 Part: 1 p: 1223 -1226, March 2001

K. Berggren, D. Nakada, T.P. Orlando, E. Macedo, R. Slattery, and T. Weir, "An integrated superconductive device technology for qubit control," submitted for publication.

T.P. Orlando, L. Tian, S. Lloyd et al, "Engineering of Measurement Induced Noise", to appear in *Physica C*, (2001);

L. Tian, S. Lloyd and T.P. Orlando, "Decoherence and Relaxation of Superconducting Persistent-Current Qubit During Measurement ", accepted by *Phys. Rev. B.* (2002);

L. Tian, S. Lloyd and T.P. Orlando, "Environmental Noise on a Qubit Through Entanglement with a Quantum Circuit", submitted to ICQI, June 2001.

L. Tian and S. Lloyd, "Resonant cancellation of off-resonant effects in a multilevel qubit", *Phys. Rev. A* 62, RC050301 (2000);

7. Scientific Personnel

The scientific personnel supported by the grant are:

1. The principal investigators: T. P. Orlando, Seth Lloyd, and J. E. Mooij. Support for Orlando is mainly a portion of his summer salary, for Lloyd is a portion of his academic salary (%5) and part of his summer salary. For Mooij the support is for living expenses during his two-month appointment as a Visiting Professor at MIT.

2. Graduate Students: This grant fully supports Lin Tian, who is working with the principal investigators and Professor Levitov in the physics department on various theoretical issues of our qubit. Lin will be graduating in June 2002. The grant supports Donald Crankshaw whose research focuses on the development of on-chip oscillators for the project as well as quantum measurement schemes. Donald will be graduating in August 2002. Daniel Nakada who was initially funded by Lincoln Laboratory is now partially funded by this grant.

3. Our effort is being coordinated with the Quantum Computation group headed by Professor Mooij at the Technical University of Delft. This grant has also benefited

greatly from the collaboration of Professor Levitov in the Theoretical Condensed Matter group in the Department of Physics as well as from Juan Mazo and Caspar van der Wal.

8. Inventions

None

9. Bibliography

None

10. Appendices

None